

# Unveiling Hidden Hardships: Leveraging Alternative Data to Map Multidimensional Vulnerability in the Central African Republic

Vincent Nossek<sup>1,2</sup>, Walker Kosmidou-Bradley<sup>1,3</sup>, Frédéric Mortier<sup>4</sup>, Bastien Cheville<sup>5</sup>, and Pierre Mandon<sup>\*1,2</sup>

<sup>1</sup>World Bank Group, Washington, D.C., USA

<sup>2</sup>CERDI & University of Clermont Auvergne, Clermont-Ferrand, France

<sup>3</sup>University of Twente, Enschede, Netherlands

<sup>4</sup>CIRAD, Montpellier, France

<sup>5</sup>Phoenix Consulting International, Paris, France

Most recent version available [here](#)  
December 11, 2025

## Abstract

In fragile states such as the Central African Republic, where conflict and institutional fragility severely constrain traditional data collection, mapping multidimensional vulnerability and potential deprivation poses a significant challenge for designing targeted interventions. This paper presents an innovative geospatial dashboard that harnesses alternative data sources—including nighttime light intensity, other relevant satellite imagery, geocoded infrastructure inventories, and critical event records—to develop high-resolution indices (at a  $5 \times 5$  km scale) of economic capacity, access to essential services (education, health, and water), flood exposure, and lethal conflict risks. By employing a Bayesian state-space model to disaggregate sectoral GDP and friction-based accessibility metrics, our analysis uncovers pronounced spatial disparities: economic activity remains concentrated in urban hubs such as Bangui, while rural areas suffer from compounded vulnerabilities, including limited economic opportunities and poor service access. Cross-validation with the 2021 Harmonized Household Living Conditions Survey confirms the predictive validity of these indices for household wealth, with economic and service indicators positively correlated with welfare outcomes. Conversely, exposure to lethal conflict appears paradoxically associated with higher-value targets, potentially reflecting rent-seeking dynamics. These tools enhance the precision of policy targeting in data-scarce environments, providing scalable and actionable insights for poverty alleviation in conflict-affected, low-income countries.

**Keywords:** Alternative data, Development economics, Fragile states, Multidimensional poverty, Satellite imagery, Conflict

**JEL Classification:** C55, I32, O12, O55, R12

---

\*Corresponding author. We thank our colleagues at the World Bank for their valuable feedback.

# 1 Introduction

Access to reliable and timely granular data is critical for effective interventions and policymaking, yet it remains extremely challenging for developing countries, particularly low-income countries (LICs) like the Central African Republic (CAR). This data scarcity stems from the prohibitive costs of traditional surveys, institutional capacity constraints, security challenges in conflict-affected regions, and insufficient technical infrastructure [Jean et al., 2016, Blumenstock, 2018]. Recent innovations utilizing alternative data sources offer promising pathways to overcome these limitations. Satellite imagery has enabled poverty mapping at unprecedented spatial resolution, as demonstrated by Jean et al. [2016], who combined nighttime luminosity (NTL) data with daytime imagery to predict local-level economic outcomes. Similarly, call detail records (CDRs) from mobile phones have facilitated measurement of population mobility patterns, economic shocks, and social network structures even in data-scarce environments [Blumenstock et al., 2015, Steele et al., 2017]. Remotely sensed vegetation indices have been utilized to monitor agricultural productivity [Burke and Lobell, 2017], while mobile money transactions have provided real-time insights into economic activity during periods when traditional data collection was impossible [Asenso-Okyere and Mekonnen, 2012]. Nevertheless, these novel methodologies face substantial challenges including algorithmic bias, representativeness concerns, and privacy considerations that necessitate careful validation against ground-truth data when available [Wesolowski et al., 2012, Blumenstock, 2018].

In CAR context, where the last comprehensive census was conducted in 2003<sup>1</sup> and where conflict has severely disrupted statistical capacity, these alternative data approaches have particular relevance. Recent empirical analysis employing the synthetic control method (SCM) yields compelling evidence regarding the disastrous economic consequences of ongoing CAR's civil war after one decade of conflict [Mandon et al., 2025].<sup>2</sup> According to the World Bank's 2023 Poverty Assessment, CAR remains one of the world's poorest nations, with approximately two-thirds of the population living below the international poverty line of US\$2.15 per day (in 2017 PPP terms). Extreme poverty is particularly concentrated in rural areas, where about 74.2 percent of households fall below the poverty threshold, compared to 61.1 percent in urban centers and 40.1 percent in Bangui, the nation's capital [World Bank, 2023]. As of end August 2025, approximately 1.1 million Central Africans remain at risk of statelessness (e.g., lack of birth registration, or the inability to prove links to any state), including around 442,000 internally displaced persons (IDPs) and 669,000 refugees in neighboring countries, severely compromising household resilience and exacerbating vulnerability to shocks.<sup>3</sup>

CAR's government still has limited control outside major towns.<sup>4</sup> This limited state authority renders traditional survey-based data collection not only logistically challenging but often physically dangerous for enumerators. A dashboard integrating remote sensing and geocoded data would be invaluable in this context for several reasons. To begin with, satellite-derived indicators offer near real-time monitoring of population movements, settlement patterns, and economic capacities in remote and conflict-ridden areas, enabling more informed policymaking and interventions. The temporal consistency of satellite imagery allows for the creation of panel datasets to identify trends and dynamic responses to interventions, which is particularly valuable in CAR, where traditional longitudinal surveys have been difficult to maintain [Jean et al., 2016]. Additionally, since 2022, the national statistical institute, ICASEES, has collected extensive cartographic data, mapping critical infrastructure such as schools, health facilities, water points, shops, and farms, providing an unprecedented baseline for service delivery planning and gap analysis [World Bank, 2023]. Moreover, combining multiple data streams, including Fathom's high-resolution flood risk mapping, offers critical insights for disaster preparedness.<sup>5</sup> Also, geocoded conflict event data from sources like the Armed Conflict Location &

<sup>1</sup>For further information, see the official documentation from the *Institut Centrafricain des Statistiques des Etudes Economiques et Sociales* (ICASEES) available [here](#).

<sup>2</sup>The hostilities that commenced in December 2012 have imposed substantial economic costs, with estimates indicating that the conflict precipitated a decline in GDP per capita ranging from 45.3 to 47.8 percent over the 2013-2022 period. This significant contraction translates to an aggregate GDP shortfall of US\$29.7 billion to US\$32.4 billion in purchasing power parity (PPP) terms.

<sup>3</sup>Additionally, as of end September 2025 CAR hosted around 63,000 international refugees and asylum seekers, mostly from neighboring Sudan, putting additional pressure especially on the northeastern Vakaga prefecture. For further information, see the online data from the Office of the United Nations High Commissioner for Refugees (UNHCR), available [here](#) and [here](#).

<sup>4</sup>For further information, see the online 2025 keynote from Human Right Watch, available [here](#).

<sup>5</sup>Fathom data is free of charge for CAR and 15 other climate vulnerable countries. For further information, see the official Fathom website, available [here](#).

Event Data Project (ACLED) [Raleigh et al., 2010], along with the friction surface model developed by Kosmidou-Bradley et al. [2025], can inform violence hazards for local populations. Finally, such a dashboard would enhance the government's capacity to implement recovery and peacebuilding initiatives by providing an evidence base for spatially targeted interventions in areas prioritized for restoring state authority, with the support of donor partners [World Bank, 2022].

This paper addresses two central objectives. First, it develops a spatially disaggregated composite index that integrates multiple dimensions of vulnerability and potential deprivation at a granular level, operationalized through a geospatial analytics dashboard. This methodological approach is particularly valuable in the context of severe data constraints aforementioned, where the production of subnational statistics is limited and socio-economic surveys outside the capital region are sparse, thereby enhancing the targeting efficiency of both humanitarian and development interventions in fragile settings.<sup>6</sup> It involves the development of a multidimensional spatial vulnerability framework that simultaneously assesses four critical domains:

- i) The analysis quantifies sectoral local economic capacities through a state-space model improved from Henderson et al. [2012] to account for propagation of uncertainty, and the integration of relevant daytime satellite imagery with precisely geocoded private business locations, enabling the identification of both primary and secondary & tertiary economic clusters.
- ii) It measures physical accessibility to essential public services by constructing infrastructure indices that incorporate both the spatial distribution of service delivery points and quality-adjusted capacity metrics (e.g., operational status). This approach accounts for the friction surface model mentioned earlier.
- iii) It incorporates physical exposure to flood hazards, a dimension of particular relevance given the concentration of population settlements along riverine corridors, most notably in Bangui.
- iv) It evaluates physical exposure to lethal conflict risk through spatiotemporal analysis of historical event patterns and the implementation of the friction surface model.

Second, the paper leverages the 2021 Harmonized Household Living Conditions Survey (*Enquête Harmonisée sur le Conditions de Vie des Ménages*, EHCVM)—the only comprehensive socio-economic household survey implemented since the onset of civil war in December 2012—to analyze welfare dynamics across heterogeneous population segments, including IDPs. This allows us to cross-check the reliability of the proposed dashboard against one of the few nationally representative and relevant surveys available.<sup>7</sup>

This paper yields three principal empirical findings. First, the multidimensional vulnerability assessment reveals pronounced spatial inequalities across CAR, with economic activity largely concentrated in Bangui while vast rural areas exhibit minimal economic presence and severely constrained access to essential services. Cross-validation using the 2021 EHCVM demonstrates strong predictive validity for our satellite-derived indices, with GDP and service access measures exhibiting consistently positive associations with household wealth at least at the 1 percent significance level. Primary-sector GDP remains positively associated with household wealth, while secondary and tertiary sectors lose significance once fixed effects are included, likely reflecting their concentration in a few urban areas, primarily Bangui.

Second, the analysis uncovers a counterintuitive positive correlation between lethal conflict exposure and household wealth, reflecting strategic targeting by armed groups of economically valuable areas rather than protective effects of prosperity. These findings underscore the complex relationship between development and security in fragile states, where relative prosperity may paradoxically increase rather than decrease exposure to violence. Regarding flooding, the data indicate that flood exposure correlates

---

<sup>6</sup>For instance, the 2011 and 2023 World Bank Enterprise Surveys (WBES), including the related Informal Sector Enterprise Survey (ISES) and Survey of Micro Firms (ESM), cover exclusively Bangui and Berbérati (i.e., the third-largest city after Bimbo). For further information, see the WBES data catalog, available [here](#).

<sup>7</sup>Conducted in 2021 by ICASEES, the survey aimed to reach 6,000 households nationally and an additional 600 households in IDP sites. The national statistical institute received official support from the Ministry of Economics, Planning, and International Cooperation (MEPIC), along with technical and financial support from the Joint Data Center on Forced Displacement, UNHCR, and the World Bank. For further information, refer to the World Bank's Poverty Assessment [World Bank, 2023].

with wealth primarily through administrative-level factors (e.g., Bangui’s effect) rather than localized, fine-grained variations.

Third, the methodological framework successfully bridges the gap between alternative data sources and ground-truth welfare outcomes, providing a scalable template for monitoring multidimensional vulnerability in data-scarce environments. The  $5 \times 5$  kilometer resolution enables identification of potential deprivation hotspots that would be obscured by traditional administrative-unit analyses, while the standardized grid system ensures replicability across diverse analytical contexts.

The remainder of this paper proceeds as follows. Section 2 establishes the empirical context of CAR’s extreme fragility and data constraints. Section 3 details the methodological approach, including an extensive discussion on the Bayesian state-space model for GDP disaggregation, as well as more succinct development on the construction of infrastructure accessibility and risk exposure indices. Section 4 presents the spatial vulnerability dashboard and validates the indices against household survey data. Section 5 discusses policy implications and broader applicability to other fragile states.

## 2 Context

CAR exemplifies the interplay between extreme deprivation and the urgent need for innovative data solutions in fragile, low-income settings. Decades of political instability, marked by recurrent coups and civil conflict since independence in 1960, have entrenched CAR as one of the world’s poorest nations [World Bank, 2022]. The economy, heavily reliant on rainfed subsistence agriculture, local agro-processing, and the retail and wholesale of imported products (e.g., food items, petroleum products), suffers from severely limited diversification and pervasive mismanagement. With a limited official export basket overwhelmingly composed of four products (i.e., diamond, gold, logs, and sawnwood), resource wealth is often channeled into embezzlement and ad-hoc arrangements with external actors (e.g., Lebanese diaspora, Rwanda, Wagner group) rather than development. Weak administration, characterized by corruption and constrained state capacity, further impedes the provision of essential services—education, healthcare, and infrastructure—leaving rural populations particularly isolated. According to the World Bank’s Poverty Assessment [World Bank, 2023], approximately two-thirds of CAR’s population survives below the international poverty line of US\$2.15 per day, with rural poverty rates reaching 74.2 percent, starkly higher than the 40.1 percent in Bangui. This multidimensional vulnerability, compounded by recurrent shocks such as armed violence and climate hazards (e.g., flooding), positions CAR as a critical case for studying poverty dynamics in environments where traditional data systems falter.

Data scarcity in CAR poses a formidable barrier to understanding and addressing this vulnerability. Persistent insecurity and logistical constraints render conventional household surveys sporadic, with the last comprehensive census dating to 2003. This absence of granular, timely data obscures subnational disparities, particularly in conflict-ridden and remote regions where poverty is most severe. Traditional statistical methods, hampered by limited state authority beyond urban centers, fail to capture the spatial and temporal heterogeneity of socio-economic conditions. The 2021 EHCVM stands as a rare exception, yet its scope remains insufficient for ongoing monitoring or localized policy design, without complementary updated information. Consequently, alternative data sources—satellite imagery, and geospatial analytics—emerge as vital tools to bridge these gaps, offering high-resolution insights into economic capacity, service access, and vulnerability to shocks.

CAR’s extreme conditions not only necessitate these data innovations but also provide a unique testing ground for refining them. The development of a spatially disaggregated composite index, as outlined in the introduction, exemplifies this potential, combining economic capacity, service access, and exposure to hazards into a multidimensional framework. Such tools, operationalized through geospatial dashboards, empower policymakers to prioritize recovery efforts in regions where state authority is weakest, aligning with donor-supported peacebuilding initiatives. By dissecting the interplay of conflict, governance failures, and economic stagnation, research in CAR yields insights that extend beyond its borders, informing strategies for poverty alleviation in other low-capacity states. Thus, CAR stands as a pivotal case for advancing data-driven approaches to vulnerability and potential deprivation, reshaping how economists measure and address poverty in the world’s most challenging environments.

### 3 Data and methodology

#### 3.1 Estimating local economic capacities

##### 3.1.1 State-space model

This study employs a state-space framework to link national GDP with its sectoral components since 1960. National GDP in logarithmic scale is denoted  $y_t$ , while  $y_{1,t}$ ,  $y_{2,t}$ , and  $y_{3,t}$  represent the primary, secondary, and tertiary sectors, and  $y_{4,t}$  refers to taxes on production. The true (latent) value of each component is  $y_{s,t}^*$  for  $s \in \{1, 2, 3, 4\}$ .

Observed quantities are related to latent sectoral GDPs through:

$$y_t = \sum_{s=1}^4 \pi_s y_{s,t}^* + \nu_t, \quad (1)$$

$$y_{s,t} = y_{s,t}^* + \omega_{s,t}, \quad s = 1, \dots, 4, \quad (2)$$

$$\ell_t = \alpha \sum_{s=1}^4 y_{s,t}^* + v_t, \quad (3)$$

where  $\pi_s$  are unknown sectoral weights in national GDP, and  $\alpha$  captures the elasticity between NTLs and economic activity [Henderson et al., 2012, Guerrero and Mendoza, 2019]. Errors  $\nu_t, \omega_{s,t}, v_t$  are independent Gaussian variables with unknown variances. Sectoral GDPs evolve as random walks:

$$y_{s,t}^* = y_{s,t-1}^* + \varepsilon_{s,t}, \quad s = 1, \dots, 4. \quad (4)$$

##### Estimation and predictions

Estimation is fully Bayesian, combining expert knowledge with uncertainty propagation. Sectoral weights follow a Dirichlet prior:

$$\pi \sim \mathcal{D}(60, 25, 15),$$

encoding prior beliefs that, structurally, GDP derives mainly from the primary sector (60 percent), followed by the secondary (25 percent), tertiary (15 percent), and taxes (10 percent). The elasticity  $\alpha$  has a Gaussian prior centered at zero with precision 10, and all variance parameters receive weakly informative inverse-Gamma priors  $\mathcal{IG}(0.001, 0.001)$ . Posterior inference is implemented in `Rjags` [Plummer, 2023], using four chains of 50,000 iterations (5,000 burn-in, thinning factor 5). Convergence diagnostics (Gelman–Rubin statistics) are below 1.01 for all key parameters.

Predictions are drawn from the posterior predictive distribution, which integrates uncertainty from states, process noise, observation noise, and parameters. For horizon  $h$ , the predictive variance of national GDP can be decomposed as:

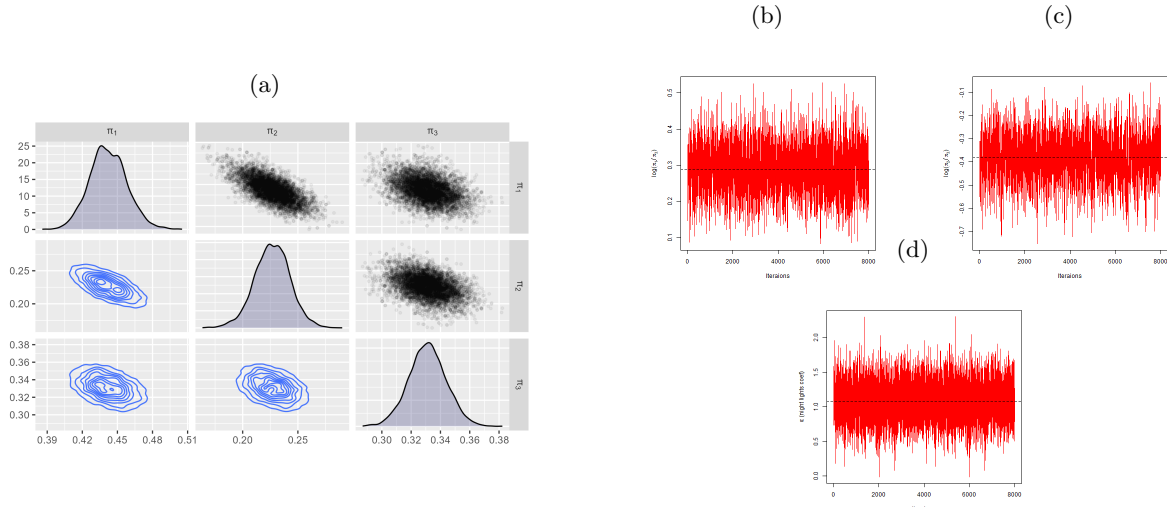
$$\begin{aligned} \text{Var}(y_{T+h} | \mathcal{D}) &= \underbrace{\pi^\top P_T \pi}_{\text{uncertainty on latent states}} \\ &+ \underbrace{h \pi^\top Q \pi}_{\text{accumulated process noise}} \\ &+ \underbrace{\sigma_\nu^2}_{\text{observation noise}} \\ &+ \underbrace{\text{Var}_{\pi, Q, \sigma_\nu^2}[\cdot]}_{\text{parameter uncertainty}} \end{aligned} \quad (5)$$

where  $P_T$  is the posterior covariance of latent sectoral GDP at time  $T$ , and  $Q$  the variance of sectoral shocks. This decomposition highlights that credible intervals widen with the forecast horizon not only because of state and observation errors, but also due to the accumulation of process uncertainty and the propagation of parameter uncertainty.

## Estimation

Posterior estimation of sector contributions to national GDP equals 42, 22, 31, and 5 percent for the primary, secondary, tertiary sectors, and taxes, respectively (see Figure 1). The secondary sector, with a contribution of 22 percent—less than the tertiary sector—might appear elevated for a sub-Saharan African country, but it is mostly driven by limited processing of raw materials, especially agricultural products.<sup>8</sup>

Figure 1: Posterior samples of sectoral GDP weights ( $\pi_1, \pi_2, \pi_3$ ).



*Source:* Authors' construction. *Notes:* Scatterplots above the diagonal show pairwise relationships between the primary, secondary, and tertiary sector weights. Below the diagonal, joint densities highlight correlations, while the diagonal displays marginal posterior densities for each parameter. These samples are drawn from the Bayesian posterior distribution, incorporating state, process, observation, and parameter uncertainties.

## Predictions

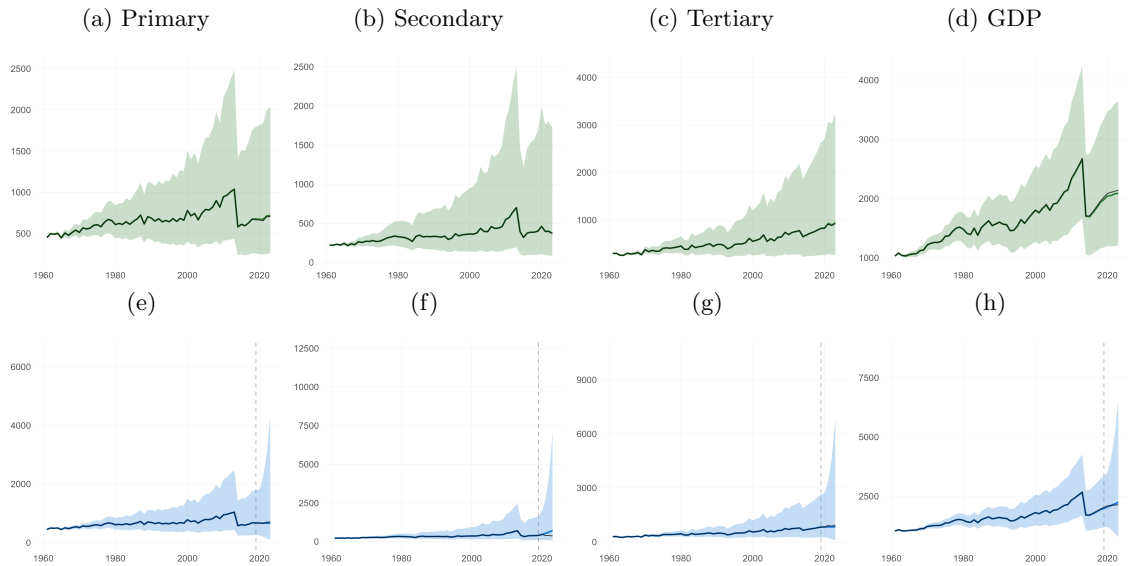
Two prediction strategies are implemented to assess model performance. The first approach employs *smoothed estimates*, which incorporate all available observations (1961–2022) to produce posterior state estimates at each time point. This yields the most accurate retrospective assessment of sectoral GDP dynamics, as the Kalman smoother integrates information from both past and future observations relative to any given time  $t$ . Credible intervals in this case reflect primarily parameter uncertainty and measurement error, as state uncertainty is minimized through the use of the complete data series.

The second approach implements *out-of-sample forecasting* to evaluate predictive validity. The model is estimated using only data from 1961–2019, and forecasts are generated for the holdout period 2020–2022. This recursive forecasting exercise starts from the last observed state in 2019 and propagates forward without incorporating subsequent observations, thereby accumulating both process noise and state uncertainty over the forecast horizon. As expected, credible intervals widen substantially in the out-of-sample predictions (Figure 2, panels e–h) compared to smoothed estimates (panels a–d), reflecting the compounding effects of parameter uncertainty, process variability, and the absence of data-based state corrections. This validation exercise demonstrates the model's ability to generate plausible short-term forecasts while acknowledging increased uncertainty for unobserved periods.

---

<sup>8</sup>According to ICASEES, the secondary sector in CAR is largely driven by local agro-processing (e.g., breweries, beverage and food processing, cigarettes, soap production). Official national accounts data are available [here](#).

Figure 2: State-space model predictions. Panels (a)–(d): smoothed estimates using all observations (1961–2022). Panels (e)–(h): out-of-sample forecasts (trained on 1961–2019, forecasted 2020–2022).



*Source:* Authors' construction. *Notes:* Shaded areas represent 80% credible intervals from MCMC posterior samples. Black lines: observed values. Vertical dashed line in bottom row indicates train/test split.

### 3.1.2 GDP spatial allocation methodology

The predicted median sectoral GDP values  $y_{st}^*$  obtained from the state-space model are spatially allocated for each year using remote sensing indicators. This analysis distinguishes between the primary sector and the combined secondary and tertiary sectors based on relevant remote sensing and geocoded data sources detailed in the Section A.1 of the Appendix.

For the primary sector, the local GDP at location  $i$  and time  $t$  is calculated as:

$$y_{Prim.i,t}^* = y_{Prim.t}^* \cdot \left( \text{shareForest}_{i,t} \cdot \frac{0.05}{2} + \text{shareDeforestation}_{i,t} \cdot \frac{0.05}{2} + \text{shareCropland}_{i,t} \cdot \frac{0.625}{3} + \text{shareNDVI}_{i,t} \cdot \frac{0.625}{3} + \text{sharePopulation}_{i,t} \cdot \frac{0.625}{3} + \text{shareWater}_{i,t} \cdot 0.05 + \text{shareGrassland}_{i,t} \cdot 0.275 \right). \quad (6)$$

This allocation scheme reflects the sectoral composition of primary activities based on historical data from ICASEES, where forestry accounts for around 5 percent of primary sector activity, agriculture represents 62.5 percent, pastoral activities constitute 27.5 percent, and water-related activities (e.g., fisheries) comprise the remaining 5 percent.<sup>9</sup>

For the combined secondary and tertiary sectors, the local GDP at location  $i$  and time  $t$  is calculated as:

$$y_{Sec.Ter.i,t}^* = y_{Sec.Ter.t}^* \cdot \left( \text{shareBuiltup}_{i,t} \cdot \frac{0.975}{3} + \text{sharePopulation}_{i,t} \cdot \frac{0.975}{3} + \text{shareSMEs}_i \cdot \frac{0.975}{3} + \text{shareMines}_i \cdot 0.025 \right). \quad (7)$$

where  $y_{Sec.Ter.it}^*$  represents the sum of the predicted secondary and tertiary sector GDP for a given year. This specification assumes that mining activities account for 2.5 percent of combined secondary and tertiary sector activity, also based on historical data from ICASEES.<sup>10</sup>

Total local GDP at time  $t$ , denoted  $y_{i,t}^*$ , is computed as the sum of  $y_{Prim.i,t}^*$  and  $y_{Sec.Ter.i,t}^*$ . All local GDP estimates are normalized using a Min–Max transformation to facilitate comparison with other key components in the geospatial analytics dashboard, including access to key infrastructure and exposure to risks of flooding and lethal conflicts, as detailed below.

The spatial allocation procedure preserves the uncertainty structure implied by the underlying statistical model. All predicted GDPs,  $y_{st}^*$ , are first spatially allocated according to Equations (6) and (7), and local uncertainty is then computed as the standard deviation of sectoral GDPs (Figure 3). Most of the uncertainty in our predictions is concentrated in areas where the predicted GDP is relatively higher, namely Bangui and the western regions of the country. The local GDPs predictions for the year 2021, obtained from the strategy using past observations, serve as reference values for the vulnerability dashboard and subsequent regression analysis.

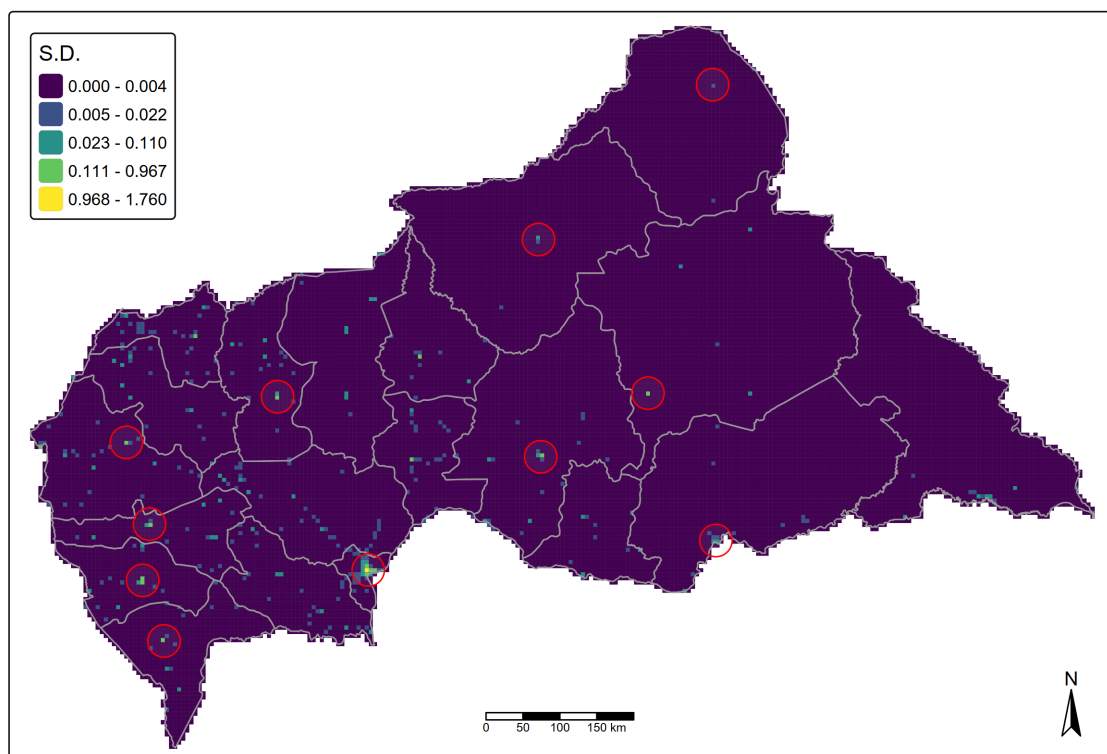
---

<sup>9</sup>Official national accounts data are available [here](#).

<sup>10</sup>Ibid. In the ICASEES framework, all extractive activities are classified within the secondary sector.

Figure 3: Local GDP uncertainty

### Standard Deviation of GDP, 2021



*Source:* Authors' construction. *Notes:* The year 2021 is used as the reference year to ensure consistency with the EHCVM survey data. For each cell we compute the Standard Deviation based on the series of all predicted local GDPs in the year 2021.

### 3.2 Assessing infrastructure access

To complement the local GDP estimates, this analysis incorporates infrastructure access measures into the dataset. The analytical strategy transforms the 100-metre WorldPop “constrained” population raster for CAR [WorldPop, 2020] into a dense lattice of points—one point for every populated cell. This approach treats each person-weighted point as the fundamental unit to which every other layer is linked. To enrich these points, contextual information at the settlement level is added to each point. These contextual variables include population totals, building counts and degree-of-urbanization classes, [Dijkstra et al., 2020] calculated/extracted to GRID3’s settlement polygons [CIESIN and Novel-T, 2021] and are tagged with the administrative codes and populations of the districts in which they fall.<sup>11</sup> The result is a single, relational table whose rows behave like households and whose attributes range from fine-scale demographics to aggregate administrative totals.

With this common reference in place, the study assesses physical accessibility to key public goods and services. ICASEES, with the support of the World Bank, provided a nationwide and comprehensive geolocated inventories of essential infrastructure, including all health facilities, primary, secondary, and tertiary schools<sup>12</sup> and water points [World Bank, 2023, 2025]. For each service type, this analysis generates nationwide travel-time surfaces using the Global High-Resolution Updatable Friction Surface (GRUFS), a pair of cost/friction raster datasets that translates on- and off-road movement into minutes of travel [Kosmidou-Bradley et al., 2025]. GRUFS Walking assumes that people are walking, even if on roads, whereas GRUFS Mixed assumes driving speeds on roads, but walking off-road. From these continuous surfaces, the methodology samples, at every population point, the shortest walking time required to reach the nearest facility of each category.<sup>13</sup> This procedure yields person-specific measures of geographic access that remain consistent across services and can be aggregated up, unweighted or population-weighted, to any spatial unit of interest, including administrative boundaries (e.g. settlement, communes, prefectures). As for the economic capacities, infrastructure access measures for education, health and water access are then normalized with a Min–Max function to allow comparisons across different service types, and geographic areas, as well as other dimensions of the dashboard.

### 3.3 Evaluating risk exposure to flooding

Flood risk assessment is incorporated using the Fathom Global 3.0 hazard model [Fathom, 2022]. Separate depth grids for fluvial and pluvial flooding were obtained for the baseline year 2020 and for future horizons under various Shared Socioeconomic Pathways (SSP), namely SSP1, SSP2, SSP3 and SSP5 in 2030, 2050 and 2080. For each time slice, this analysis considers return periods from five to one thousand years, capturing both frequent, low-impact events and rare, catastrophic ones. Maximum water depths from these scenarios were sampled at the same set of population points established in the infrastructure access assessment.

To enable comparison across time horizons and hazard types, this analysis standardizes the depth values. Processing uses Python and ArcPy via ArcGIS Pro version 3.4, with checksums recorded for reproducibility. The flood index employs the SSP2 scenario with the 2030 horizon. Flood risk measures are also normalized using a Min–Max function to facilitate comparison with other dimensions of the dashboard.<sup>14</sup>

### 3.4 Appraising risk exposure to lethal conflicts

Conflict exposure assessment recreates the Spatial Conflict Index Raster (SCIR) with the latest ACLED through December 2024. Following the kernel-density approach laid out by Gevaert and Kosmidou-Bradley [2023], this analysis produces a series of five-year rolling averages (i.e., 2015-20, 2016-21, ...

<sup>11</sup>For further information, see the documentation, available [here](#).

<sup>12</sup>The inventory encompasses both public and private health facilities and educational establishments. The dataset accounts for the operational status of each facility, distinguishing between active and inactive establishments, and considers exclusively active ones.

<sup>13</sup>The analysis in this study focuses on journeys taken on foot, as other transport modes may not be available to the poorest and most deprived people if private or public transport is unavailable or unaffordable [World Bank, 2023, p.114].

<sup>14</sup>Compared to local economic capacities and infrastructure access, higher values indicate greater flood risk exposure, reflecting more detrimental outcomes.

2019-24) alongside a raster summarizing the entire study period. Each surface represents a temporally-smoothed, fatality-weighted intensity score, in terms of standard deviations, that falls off with distance from reported events (i.e., geocoded lethal conflicts).

As with the infrastructure and flood risk assessments, values were extracted directly to the population points, ensuring that every household analogue carries a time-stamped indicator of conflict risk. This approach maintains consistency across all risk measures and enables comprehensive analysis of the relationship between economic capacities and various forms of risk exposure. Conflict exposure measures are also normalized with a Min–Max function to facilitate comparison with other dimensions of the dashboard aforementioned.<sup>15</sup>

### 3.5 Vulnerability Index

**Index of Vulnerability ( $\text{Idx\_Vulnerab\_Final}$ ).** This composite index summarizes overall vulnerability for each location (i) averaging six previously defined component indices—each oriented so that larger values mean *worse* conditions—and then (ii) rescaling the result to [0, 100] via Min–Max normalization. The six components are:  $\text{Idx\_GDP}$ ,  $\text{Idx\_educ\_prim}$ ,  $\text{Idx\_health}$ ,  $\text{Idx\_water\_access}$ ,  $\text{Idx\_conflicts}$ , and  $\text{Idx\_floods}$ .

Let  $i$  index spatial units and assume each component index  $S_{k,i} \in [0, 100]$  (higher = better for GDP and infrastructure components, worse otherwise). First, build an *unnormalized* vulnerability score by reversing the direction of GDP and infrastructure components and taking their mean:

$$V_i = \frac{1}{6} \left[ (100 - \text{Idx\_GDP}_i) + (100 - \text{Idx\_educ\_prim}_i) + (100 - \text{Idx\_health}_i) + (100 - \text{Idx\_water\_access}_i) + \text{Idx\_conflicts}_i + \text{Idx\_floods}_i \right] \quad (8)$$

Min–Max normalization is then applied across all units to obtain the final index, which is multiplied by 100:

$$\text{Idx\_Vulnerab\_Final}_i = 100 \times \frac{V_i - \min_j V_j}{\max_j V_j - \min_j V_j}. \quad (9)$$

where the minimum and maximum are computed over the full set of units  $j$ . Higher values of  $\text{Idx\_Vulnerab\_Final}$  indicate higher (worse) vulnerability and potential deprivation.

## 4 Results

### 4.1 Spatial vulnerability dashboard

This section presents the spatial dashboard constructed through multi-dimensional indexing aforementioned at an unprecedented granular scale for CAR. The dashboard employs a standardized grid-cell approach with  $5 \times 5$  km resolution, providing a replicable and scalable methodological framework that represents a significant advancement in spatial development analysis for fragile states in general and CAR in particular.<sup>16</sup> This granular approach enables precise identification of vulnerability hotspots and might facilitate targeted policy interventions, while the standardized grid system ensures methodological consistency and comparability across different spatial units of analysis.

The dashboard comprises an overall vulnerability index and its six core vulnerability components that cover the dimensions aforementioned: local economic capacity, access to essential services (education, health, water), and exposure to flooding and conflict-related shocks. As also previously discussed, each index is normalized on a 0-100 scale, where higher values indicate better outcomes for capacity indicators (i.e., GDP and infrastructure components) and higher exposure for risk indicators. The spatial resolution adopted here provides critical advantages over traditional administrative-unit analyses, as it captures intra-regional heterogeneity and enables identification of localized vulnerability and potential deprivation patterns that would otherwise be obscured by administrative aggregation.

---

<sup>15</sup>As with flood risk exposure, higher values reflect more detrimental outcomes.

<sup>16</sup>The replication material is available [here](#).

Importantly, this methodological framework is fully adaptable to alternative spatial units of interest, from administrative boundaries to custom-defined zones, ensuring broad applicability across diverse analytical contexts. Section A.2 of the Appendix presents each dimension at the communal administrative (admin 3) level, showing which communes overperform or underperform relative to the national median of each component.

The composite vulnerability index reveals pronounced spatial heterogeneity in development challenges across the Central African Republic (Figure 4). Bangui and its surrounding areas appear relatively less vulnerable than the rest of the country, forming the only substantial region in the 0–24 range despite periodic exposure to lethal conflicts and flooding.<sup>17</sup> Western remote regions—particularly areas around Berbérati, Bouar, and the southwestern prefectures—exhibit high composite vulnerability scores (75–100 range), indicated by the dark red shading. The concentration of elevated vulnerability in these western areas likely reflects the compound nature of development challenges in zones distant from the capital and simultaneously constrained by infrastructure deficits. The central corridor extending from Bangui through Bambari and Bouar displays intermediate (25–49) to high (50–74) vulnerability levels, shown in pale green and orange. Although these areas benefit from somewhat better economic connectivity and service infrastructure than the most vulnerable regions, persistent conflict exposure substantially heightens overall vulnerability. The spatial pattern suggests that proximity to major transport routes and urban centers provides only partial protection when conflict risks remain high. The northeastern and eastern regions exhibit more spatially dispersed vulnerability, with clusters of extreme vulnerability interspersed with largely uninhabited areas. Low population density in these zones creates distinct vulnerability dynamics, where the combination of remoteness, limited service infrastructure, and periodic exposure to lethal conflicts and climate hazards generates localized vulnerability hotspots.

Figures 5 through 8 present the spatial distribution of economic capacity and access to fundamental public services across CAR at the grid level. The total GDP index reveals a highly concentrated economic geography, with Bangui and its immediate periphery exhibiting the highest economic activity levels (index values exceeding 65), while vast rural areas display minimal economic activity (index values below 7.7).<sup>18</sup> This stark spatial polarization underscores the capital-centric nature of the small economic activity in CAR,<sup>19</sup> with secondary urban centers such as Bambari, Berbérati, and Bouar showing very modest economic activity clusters.

The education access landscape demonstrates greater spatial coverage than economic activity, with numerous areas achieving high primary education access scores (67–100 range), especially in the central part of the country and close to transportation corridors. By contrast, western remote areas and northeastern territories show more limited coverage. This pattern suggests that educational service provision has achieved broader geographic penetration than economic development, though significant gaps remain in peripheral areas.

Healthcare access presents a more constrained spatial distribution, with the majority of the territory falling within the lowest accessibility categories (0–29 range). Urban centers and their immediate surroundings demonstrate the highest health service accessibility, while extensive rural areas face severe healthcare access constraints. This spatial pattern indicates substantial geographic inequities in healthcare provision, with potential implications for population health outcomes, human capital development as well as social discontent stemming from likely relative deprivation.

Water access exhibits an intermediate spatial distribution pattern, with better coverage than healthcare but more limited than education. The distribution reveals clusters of high accessibility around major urban centers and along major transportation corridors, while remote areas, particularly in the eastern parts of CAR, show very limited water infrastructure access.

Figures 9 and 10 present the spatial distribution of environmental and conflict-related vulnerability exposures. The flooding exposure index reveals highly localized risk patterns, with elevated exposure concentrated along major river systems, particularly the Ubangi River corridor and its tributaries. Bangui faces particularly acute flood exposure given its riverside location, while cities such as Bambari, Berbérati, Birao, Bria, and Nola exhibit significant flood vulnerability. The concentrated nature of

---

<sup>17</sup>This assessment is relative to the national context, Bangui and surroundings remain highly deprived in comparison with international standards [World Bank, 2022, 2023].

<sup>18</sup>The split between primary GDP activities and secondary/tertiary activities is available in the Section A.2 of the Appendix.

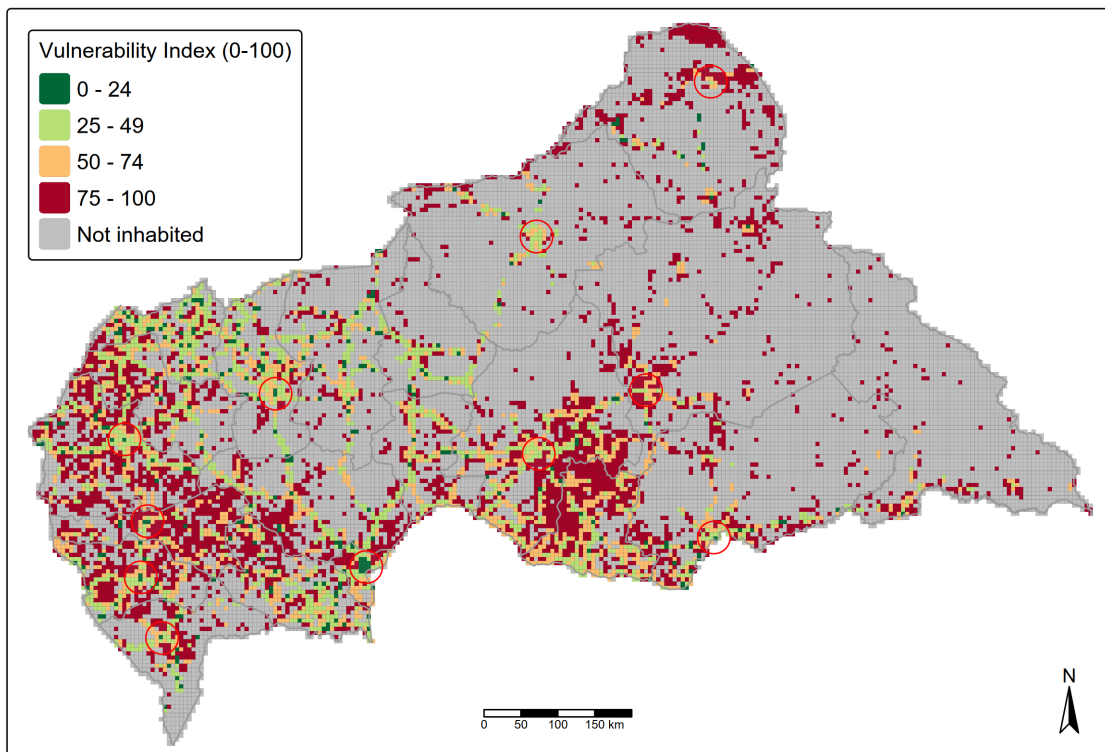
<sup>19</sup>Based on the state space model the total GDP in CAR was around US\$1,890 million on average in 2021, when the EHCVM was finalized.

flood risk enables targeted flood management interventions in high-exposure areas.<sup>20</sup>

Lethal conflict exposure over the years demonstrates a markedly different spatial pattern, with widespread distribution across the national territory and notable concentrations in strategically important locations. Major urban centers including Bambari, the capital city Bangui, Bangassou, and Bria, exhibit particularly high lethal conflict exposure indices, reflecting the complex interaction between population density, (political) rent capture, resource competition, and political instability. The extensive geographic spread of lethal conflict exposure underscores the pervasive nature of security challenges in CAR and the need for comprehensive conflict-sensitive development approaches.<sup>21</sup>

Figure 4: Overall vulnerability index at granular level

### Overall vulnerability

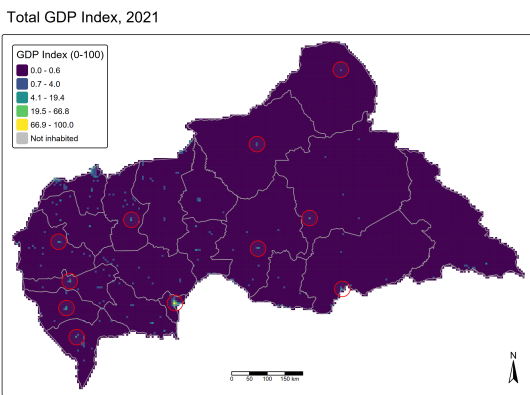


*Source:* Authors' construction. *Notes:* Standardized grid-cell approach with 5×5 km resolution. The composite vulnerability index ranges from 0 to 100, with higher values indicating greater vulnerability (100 = most vulnerable; 0 = least vulnerable, relative to national standards). Gray areas on the map represent regions with no reported population. Red circles indicate Bangui and the ten subsequent major urban centers in CAR.

<sup>20</sup>For instance, one primary objective of the World Bank's Provir project (started in 2023) is the management of flood and erosion risk protection in key urban centers, including Bangui and Berbérati. For further information, see the official press release from the World Bank, available [here](#).

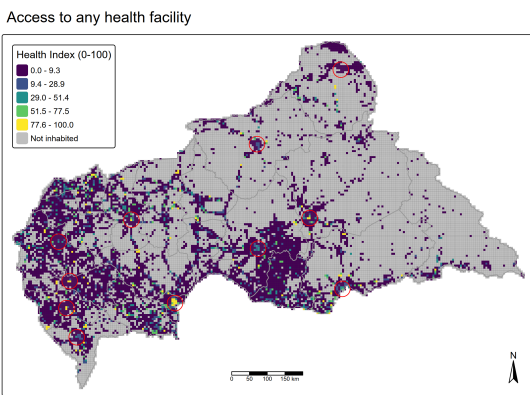
<sup>21</sup>For instance, the World Bank's Local Governance and Community Resilience Project (started in 2023) For further information, see the project appraisal document, available [here](#).

Figure 5: GDP index



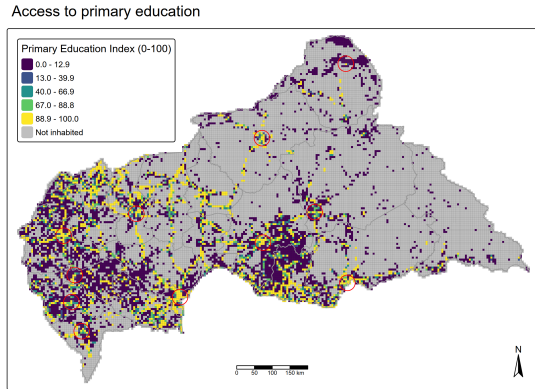
*Source:* Authors' construction. *Notes:* Standardized grid-cell approach with  $5 \times 5$  km resolution. The year 2021 is used as the reference year to ensure consistency with the EHCVM survey data. Economic activity concentration measured through relevant remote sensing and geocoded data. Index ranges from 0 (minimal economic activity) to 100 (maximum economic density). Red circles indicate Bangui and the ten subsequent major urban centers in CAR. Intervals are computed using Fisher grouping method.

Figure 7: Health access index



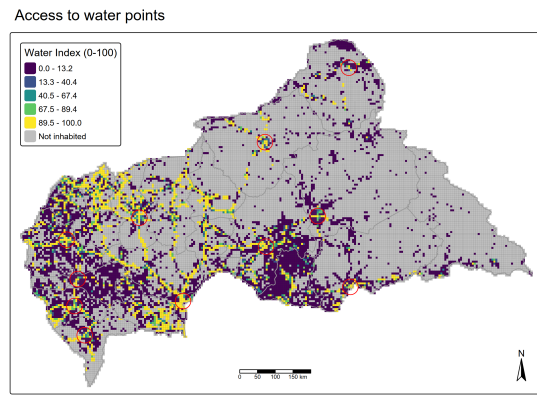
*Source:* Authors' construction. *Notes:* Standardized grid-cell approach with  $5 \times 5$  km resolution. Proximity and accessibility to any health facilities. Index reflects travel time and service availability, with higher values indicating better healthcare access. Gray areas on the map represent regions with no reported population. Red circles indicate Bangui and the ten subsequent major urban centers in CAR. Intervals are computed using Fisher grouping method.

Figure 6: Education access index



*Source:* Authors' construction. *Notes:* Standardized grid-cell approach with  $5 \times 5$  km resolution. Spatial accessibility to all primary education facilities based on travel time and infrastructure density. Higher values indicate better educational access. Gray areas on the map represent regions with no reported population. Red circles indicate Bangui and the ten subsequent major urban centers in CAR. Intervals are computed using Fisher grouping method.

Figure 8: Water access index



*Source:* Authors' construction. *Notes:* Standardized grid-cell approach with  $5 \times 5$  km resolution. Spatial distribution of water point accessibility and infrastructure coverage. Higher values represent better water access conditions. Gray areas on the map represent regions with no reported population. Red circles indicate Bangui and the ten subsequent major urban centers in CAR. Intervals are computed using Fisher grouping method.

Figure 9: Floods index

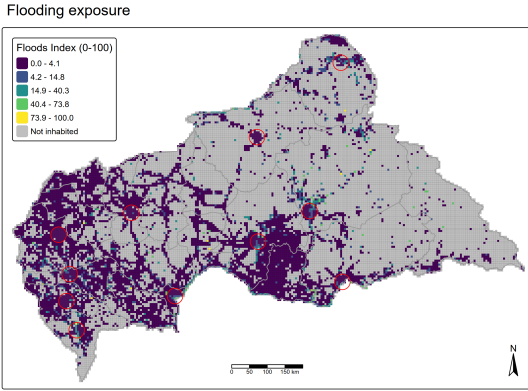
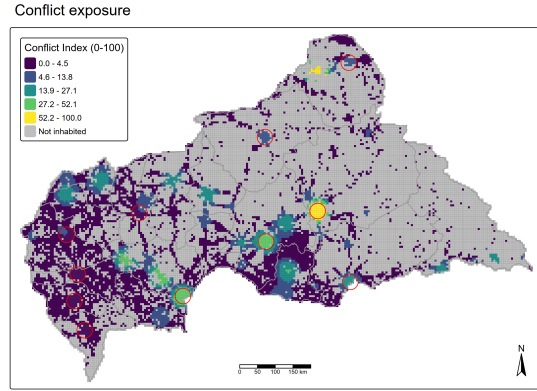


Figure 10: Conflict index



*Source:* Authors' construction. *Notes:* Standardized grid-cell approach with  $5 \times 5$  km resolution. Spatial vulnerability to flood events based on topographical, hydrological, and historical flood data. Higher values indicate greater flood exposure risk. Gray areas on the map represent regions with no reported population. Red circles indicate Bangui and the ten subsequent major urban centers in CAR. Intervals are computed using Fisher grouping method.

*Source:* Authors' construction. *Notes:* Standardized grid-cell approach with  $5 \times 5$  km resolution. The period 2016-21 (rolling average) is used as a reference to ensure consistency with the EHCVM survey data. Spatial distribution of conflict risk based on historical incident data and proximity to lethal conflict zones. Higher values represent greater lethal conflict exposure, with notable concentrations in urban centers and strategic locations. Gray areas on the map represent regions with no reported population. Red circles indicate Bangui and the ten subsequent major urban centers in CAR. Intervals are computed using Fisher grouping method.

## 4.2 Cross-validation with household survey data

### 4.2.1 Empirical strategy

To validate the spatial vulnerability indices developed in this analysis, cross-validation is employed using household-level data from the EHCVM 2021. Household wealth indices are constructed following the standardized Demographic and Health Surveys (DHS) methodology<sup>22</sup>. Households are then spatially matched to their corresponding  $5 \times 5$  kilometer grid cells to examine the relationship between the spatial indices and household-level welfare outcomes. The empirical specification takes the following form:

$$W_{i,g} = \alpha + \beta_1 GDP_g + \beta_2 Education_g + \beta_3 Health_g + \beta_4 Water_g + \gamma X_{i,g} + \delta_r + \epsilon_{i,g} \quad (10)$$

where  $W_{i,g}$  represents the wealth index for household  $i$  located in grid cell  $g$ ,  $GDP_g$  denotes the economic activity index for grid cell  $g$ , which can alternatively be decomposed into primary activities and secondary/tertiary activities, and  $Education_g$ ,  $Health_g$ , and  $Water_g$  represent the respective service access indices. The vector  $X_{i,g}$  captures household-level control variables,<sup>23</sup>  $\delta_r$  represents regional or prefectoral fixed effects, and  $\epsilon_{i,g}$  is the error term. When explicitly indicated, standard errors are clustered at the prefectoral level to account for spatial correlation. The high spatial resolution of our indices enables identification from within-administrative variation in local conditions.

<sup>22</sup>For further information, see the official documentation from the DHS available [here](#).

<sup>23</sup>The selection of household-level controls  $X_{i,g}$  is derived from the World Bank's Poverty Assessment [World Bank, 2023]. It includes demographic characteristics (i.e., household size, age and gender of household head), human capital variables (i.e., educational attainment of household head), employment sector indicators (i.e., sectoral activity of household head), and displacement status (i.e., IDPs in ordinary households or in refugee camps).

For shock exposure analysis, the following slightly alternative specification is estimated:

$$W_{i,g} = \alpha + \beta_1 GDP_g + \beta_2 Floods_g + \beta_3 Conflicts_g + \gamma X_{i,g} + \delta_r + \epsilon_{i,g} \quad (11)$$

where  $Floods_g$  and  $Conflicts_g$  represent exposure indices for environmental and conflict-related risks respectively.<sup>24</sup>

#### 4.2.2 Validation results for economic capacity and service access

Table 1 presents the validation results for economic capacity and basic service access indices. The findings provide strong empirical support for the spatial vulnerability framework developed in this study. The GDP index demonstrates a robust positive and statistically significant association with household wealth across all specifications. This relationship remains statistically significant at the 1 or 0.1 percent level even after controlling for regional and prefectoral fixed effects, confirming that areas with higher local economic activity as measured through relevant remote sensing and geocoded data effectively correspond to higher household welfare levels.

The three service access indices display consistently positive and significant associations with household wealth, though somewhat weaker for health access, confirming their relevance as welfare predictors. The robustness of these results across alternative fixed-effects specifications further strengthens the credibility of the spatial indices. In particular, the inclusion of prefectoral fixed effects with clustered standard errors (Column 3) accounts for unobserved heterogeneity at a key administrative level. Although this specification reduces the magnitude of the coefficients, their statistical significance persists, indicating that the indices capture local variation beyond broader administrative attributes.<sup>25</sup>

Tables A.2 and A.3 in the Section A.3 of the Appendix report results with GDP disaggregated by sector. Primary-sector GDP is significantly and positively associated with household wealth, whereas the secondary and tertiary sectors lose significance once different levels of fixed effects are introduced. This pattern likely reflects the spatial concentration of secondary and tertiary activities in a few areas—chiefly Bangui—whereas primary activities, particularly subsistence agriculture, are more widely distributed across the country [World Bank, 2022].

---

<sup>24</sup>Both  $GDP_g$  and  $Conflicts_g$  have panel dimensions but are reported with respectively 2021 and 2016-21 (rolling average) as reference years to ensure consistency with the EHCVM survey data.

<sup>25</sup>As of 2025, in both legal frameworks and practical applications, prefectures continue to hold greater relevance and authority than communes in the exercise of routine state functions, security measures, and inter-ministerial coordination beyond Bangui. The operational capacities of communes are markedly limited by insufficient decentralization and a severe lack of resources [World Bank, 2025].

Table 1: Spatial vulnerability indices and household wealth: Basic Services and economic activity

	Households' baseline wealth index		
	Col.1	Col.2	Col.3
GDP	0.098*** (0.007)	0.049** (0.010)	0.048*** (0.010)
Access to health index	0.014*** (0.002)	0.004 (0.002)	0.005* (0.002)
Access to primary education index	0.005*** (0.001)	0.006** (0.001)	0.005** (0.001)
Access to water index	0.013*** (0.001)	0.012*** (0.001)	0.011*** (0.001)
R2 Adj.	0.443	0.462	0.463
Num.Obs.	6,264	6,264	6,264
Covariates	Yes	Yes	Yes
Fixed effects	No	Regional	Prefectoral
Clustered standard errors	No	Yes	Yes

\* p < 0.05, \*\* p < 0.01, \*\*\* p < 0.001

*Source:* Authors' construction. *Notes:* Dependent variable is the household wealth index constructed following DHS methodology using EHCVM 2021 data. All spatial indices are measured at 5×5 km grid cell level and normalized on 0-100 scale. The GDP index is constructed using relevant remote sensing and geocoded data. Service access indices are derived from travel time to facilities and the density of associated infrastructure. Higher values mean higher local economic activities or better service access. Additional covariates—household (HH) size; presence of IDPs in ordinary households or camps; whether the HH head is a woman; HH head's education level (primary, secondary first cycle, secondary second cycle, or higher); age of the HH head; and HH employment status (secondary sector, tertiary sector, or inactive/unemployed)—are included as controls but omitted from the table for brevity. Regional fixed effects account for the seven administrative regions of CAR, and prefectoral fixed effects control for the 20 prefectures. Standard errors are clustered at the regional level in Column (2) and the prefectoral level in Column (3). The sample comprises 6,264 households spatially matched to grid cells.

#### 4.2.3 Shock exposure validation

Table 2 examines the relationship between spatial vulnerability indices and household wealth in the context of environmental and conflict-related exposures. The lethal conflict exposure index exhibits a positive and statistically significant association with household wealth, a finding that initially appears counterintuitive but reflects important conflict dynamics in fragile states. The coefficient indicates that areas with higher conflict exposure paradoxically correspond to higher household wealth levels.

This seemingly paradoxical relationship likely reflects the strategic targeting behavior of armed groups against the state, its allies and proxies over the past decade, who concentrate activities in economically valuable areas including urban centers, mining regions, and areas with valuable natural resources or infrastructure [Buhaug and Rød, 2006, Berman et al., 2017]. Rather than indicating that conflict improves welfare, this relationship plausibly demonstrates that (relative) wealth concentration creates attractive targets for armed groups, generating the positive spatial correlation between lethal conflict exposure and economic activity. This finding underscores the complex relationship between economic development and security in fragile states [Laville and Mandon, 2025], where even relative prosperity may increase rather than decrease exposure to conflict risks. By contrast, the flooding exposure index shows no statistically significant association with household wealth.

Table 2: Spatial vulnerability indices and household wealth: Shock exposure and economic activity

	Households' wealth index		
	Col.1	Col.2	Col.3
GDP	0.095*** (0.007)	0.048** (0.010)	0.047*** (0.010)
Floods index	0.026 (0.018)	0.004 (0.019)	0.012 (0.020)
Conflicts index	0.038*** (0.005)	0.029*** (0.004)	0.037*** (0.005)
R2 Adj.	0.442	0.461	0.463
Num.Obs.	6,264	6,264	6,264
Covariates	Yes	Yes	Yes
Fixed effects	No	Regional	Prefectoral
Clustered standard errors	No	Yes	Yes

\* p < 0.05, \*\* p < 0.01, \*\*\* p < 0.001

*Source:* Authors' construction. *Notes:* Dependent variable is the household wealth index constructed following DHS methodology using EHCVM 2021 data. All spatial indices are measured at 5×5 km grid cell level and normalized on 0-100 scale. The GDP index is constructed from remote sensing and geocoded data. The risk indices measure physical exposure to flooding and lethal conflict, incorporating travel time to (potential) events. Higher values mean higher local economic activities or better service access. Additional covariates—HH size; presence of IDPs in ordinary households or camps; whether the HH head is a woman; HH head's education level (primary, secondary first cycle, secondary second cycle, or higher); age of the HH head; and HH employment status (secondary sector, tertiary sector, or inactive/unemployed)—are included as controls but omitted from the table for brevity. Regional fixed effects account for the seven administrative regions of CAR, and prefectoral fixed effects control for the 20 prefectures. Standard errors are clustered at the regional level in Column (2) and the prefectoral level in Column (3). The sample comprises 6,264 households spatially matched to grid cells.

#### 4.2.4 Robustness checks on wealth measurement

Tables A.4 and A.5 in Section A.3 of the Appendix report an alternative computation of the wealth index following the DHS methodology. This approach applies distinct procedures for urban and rural households<sup>26</sup> and confirms the robustness of the baseline results in both magnitude and statistical significance.

## 5 Discussion

The multidimensional vulnerability assessment in this paper integrates a Bayesian state-space model, friction-based accessibility metrics, and relevant remote sensing and geocoded data. It reveals stark spatial inequalities across CAR. The modest economic activity concentrates heavily in Bangui and its periphery, while vast rural areas exhibit minimal economic presence. Service access patterns vary markedly across sectors. Education exhibits relatively broad geographic coverage, with many areas—particularly in the central part of the country, which is comparatively better connected by road networks—achieving high access scores to primary schools. Healthcare access remains severely constrained, with most of the territory falling into the lowest accessibility categories. Water access shows intermediate coverage, concentrated around urban centers and along main transportation corridors.

Risk exposure analysis uncovers distinct spatial patterns for different hazards. Flooding exposure concentrates along major river systems, particularly affecting Bangui and cities such as Bambari, Berbérati, Birao, Bria, and Nola. Lethal conflict exposure demonstrates widespread distribution across the national territory with notable concentrations in strategically important urban centers including Bambari, Bangui, Bangassou, and Bria.

The cross-validation exercise provides strong empirical support for the indices derived from state space model, as well as relevant remote sensing and geocoded data. Local economic activity estimates and all service access measures—education, health, and water—exhibit consistently positive and significant relationships with household wealth. Primary-sector GDP remains positively associated with household wealth, whereas secondary and tertiary sectors lose significance once fixed effects are applied, consistent with their urban concentration, mostly in Bangui, and the widespread nature

<sup>26</sup>As for the baseline wealth index, see the official documentation from the DHS available [here](#).

of primary activities. Moreover, the analysis reveals a counterintuitive positive correlation between lethal conflict exposure and household wealth, reflecting strategic targeting of economically valuable areas by armed groups rather than protective effects of prosperity [Buhaug and Rød, 2006, Berman et al., 2017]. Regarding flooding, the data indicate that flood exposure correlates with wealth primarily through administrative-level factors (e.g., Bangui's effect) rather than localized, fine-grained variations.

These findings have immediate policy implications for CAR and broader applicability to other fragile states. The extreme spatial polarization underscores the need for spatially differentiated development strategies that address both the concentration of economic activity and the multidimensional nature of vulnerability. The positive conflict-wealth correlation necessitates conflict-sensitive approaches to development programming that account for the security risks associated with economic activity.

The framework developed here offers a template for scaling up alternative data applications across sub-Saharan Africa and other regions where conventional statistical systems face severe capacity constraints. For instance, relatively similar approaches are currently being developed for Afghanistan and Gabon by the World Bank. By successfully bridging the gap between satellite-derived insights and ground-truth welfare outcomes, this research contributes to the growing toolkit available for monitoring progress toward sustainable development goals in the world's most vulnerable populations. As traditional data systems remain compromised by ongoing fragility, such methodological innovations become increasingly critical for evidence-based policymaking in fragile states.

## References

- K. Asenso-Okyere and D. A. Mekonnen. The importance of ICTs in the provision of information for improving agricultural productivity and rural incomes in Africa. African human development report, UNDP Regional Bureau for Africa, 2012.
- N. Berman, M. Couttenier, D. Rohner, and M. Thoenig. This mine is mine! How minerals fuel conflicts in Africa. *American Economic Review*, 107(6):1564–1610, 2017.
- J. E. Blumenstock. Don’t forget people in the use of big data for development. *Nature*, 561(7722):170–172, 2018.
- J. E. Blumenstock, G. Cadamuro, and R. On. Predicting poverty and wealth from mobile phone metadata. *Science*, 350(6264):1073–1076, 2015.
- H. Buhaug and J. K. Rød. Local determinants of African civil wars, 1970–2001. *Political Geography*, 25(3):315–335, 2006.
- M. Burke and D. B. Lobell. Satellite-based assessment of yield variation and its determinants in smallholder African systems. *Proceedings of the National Academy of Sciences*, 114(9):2189–2194, 2017.
- CIESIN and Novel-T. GRID3 Central African Republic settlement extents. Geo-Referenced Infrastructure and Demographic Data for Development (GRID3), 2021. Version 01.01. CIESIN: Center for International Earth Science Information Network, Columbia University.
- L. Dijkstra, T. Brandmüller, T. Kemper, A. Khan, and P. Veneri. Applying the degree of urbanisation. *Publications Office of the European Union*, 2020.
- Fathom. Fathom-Global Flood Map — version 3.0. Data set, 2022.
- C. Gevaert and W. Kosmidou-Bradley. Spatial conflict index raster. Mimeo/Unpublished manuscript, 2023.
- V. Guerrero and J. Mendoza. On measuring economic growth from outer space: A single country approach. *Empirical Economics*, 57, 2019.
- J. Vernon Henderson, Adam Storeygard, and David N. Weil. Measuring economic growth from outer space. *American Economic Review*, 102(2):994–1028, 2012.
- N. Jean, M. Burke, M. Xie, W. M. Davis, D. B. Lobell, and S. Ermon. Combining satellite imagery and machine learning to predict poverty. *Science*, 353(6301):790–794, 2016.
- W. Kosmidou-Bradley, Y. Gevaert, R. de By Dou, and A. Nelson. Introducing the global high-resolution updatable friction surface, 2025. Mimeo/Unpublished manuscript.
- C. Laville and P. Mandon. Internal conflicts and shocks: A narrative meta-analysis. *Journal of Peace Research*, 62(4):1159–1175, 2025.
- P. Mandon, V. Nossek, and D. S. Tomi. Stuck in a fragility trap: The case of the Central African Republic civil war. *Defence and Peace Economics*, 36(4):435–468, 2025.
- M. Plummer. *rjags: Bayesian Graphical Models using MCMC*, 2023. URL <https://CRAN.R-project.org/package=rjags>. R package version 4-15.
- C. Raleigh, A. Linke, H. Hegre, and J. Karlsen. Introducing ACLED: An armed conflict location and event dataset. *Journal of Peace Research*, 47(5):651–660, 2010.
- J. E. Steele, P. R. Sundsøy, C. Pezzullo, V. A. Alegana, T. J. Bird, J. E. Blumenstock, J. Bjelland, K. Engø-Monsen, Y.-A. de Montjoye, A. M. Iqbal, et al. Mapping poverty using mobile phone and satellite data. *Journal of The Royal Society Interface*, 14(127):20160690, 2017.
- A. Wesolowski, N. Eagle, A. J. Tatem, D. L. Smith, A. M. Noor, R. W. Snow, and C. O. Buckee. Quantifying the impact of human mobility on malaria. *Science*, 338(6104):267–270, 2012.

World Bank. Central African Republic Country Economic Memorandum: Paving the way out of fragility for a brighter future. Technical report, World Bank Group, Washington, DC, 2022.

World Bank. Central African Republic Poverty Assessment: A road map towards poverty reduction in the Central African Republic. Technical report, World Bank Group, Washington, DC, 2023.

World Bank. Central African Republic Public Finance Review: Enhance transparency, sustainability, and effectiveness of the public sector. Technical report, World Bank Group, Washington, DC, 2025.

WorldPop. Central African Republic constrained 100 m population. <https://www.worldpop.org>, 2020. GeoTIFF.

# Appendix

## A.1 Sources for relevant remote sensing and geocoded data

### A.1.1 Economic activity measurement

The analysis employs Defense Meteorological Satellite Program (DMSP) satellite data for long-term modeling combined with extended DMSP datasets through 2022 from the Earth Observation Group at Colorado School of Mines. Visible Infrared Imaging Radiometer Suite (VIIRS) data, while superior for rural area detection, remains unavailable before 2013 and therefore cannot support the full temporal scope required.

The analysis also incorporates complementary remote sensing indicators including population density, built-up area coverage, and infrastructure survey data from ICASEES to capture secondary and tertiary sector activities that operate without consistent electricity access.

Land cover classification data enables identification of primary economic activities through cropland delineation combined with Normalized Difference Vegetation Index (NDVI) measurements as agricultural productivity proxies. Forestry sector activities are captured through forest density indicators combined with deforestation indices to identify active logging areas. Mining sector activities utilize known industrial and artisanal mine locations for spatial allocation.

### A.1.2 Service accessibility data

Physical accessibility to essential public services relies on comprehensive facility location databases. Health center locations, primary education schools, and water point coordinates are sourced from ICASEES. These datasets enable travel time calculations and accessibility modeling for service provision analysis.

### A.1.3 Risk Exposure Data

Conflict exposure measurement utilizes ACLED records, which provide georeferenced violent event data with temporal precision. This enables spatial proximity calculations and conflict density mapping for vulnerability assessment. This paper focuses on lethal conflicts only. Flood hazard exposure employs Fathom Global 3.0 datasets, which provide comprehensive flood risk modeling incorporating topographical vulnerability and historical flood occurrence patterns. These data support identification of areas with elevated environmental risk exposure.

The comprehensive data sources and their respective spatial and temporal resolutions are detailed in Table A.1.

Table A.1: Relevant remote sensing and geocoded data sources

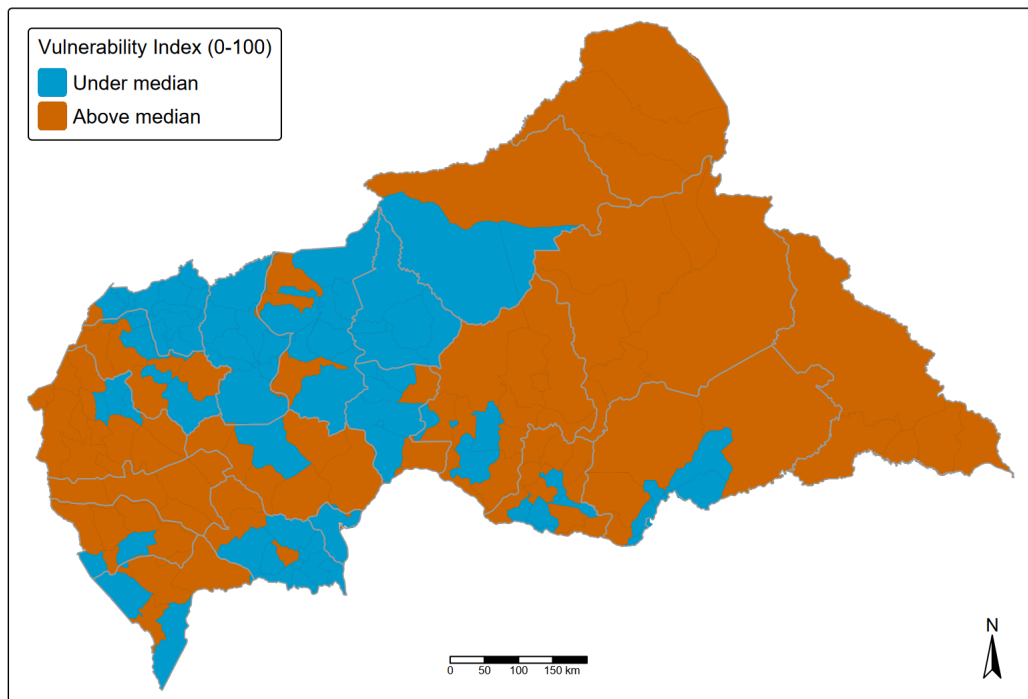
Variable	Resolution	Temporality	Source(s)
NTLs, DMSP	1000 m	1992-2022	EOG, Colorado School of Mines
NTLs, VIIRS	500 m	2013-22	EOG, Colorado School of Mines
Population	1 km	2013-21	LandScan, Oak Ridge Lab.
Land Cover (built-up, forest, etc.)	100 m	2015-19	Modis
NDVI (vegetation index)	250 m	2000-22	Modis Terra
Deforestation (forest change)	30 m	2000-22	University of Maryland
Industrial mines locations	Points	2010-19	Minex & US Geological Survey
Artisanal mines locations	Points	2019	IPIS
Private operators	Points	2023	ICASEES
Health and education facilities	Points	2023	ICASEES
Water points	Points	2023	ICASEES
Flood risk	30 m	2020-30	Fathom Global 3.0
Violent events (lethal conflicts)	Points	5yrs rw (e.g., 2016-21)	ACLED

Source: Authors' construction.

## A.2 Vulnerability at communal level

Figure A.1: Overall vulnerability index at communal level

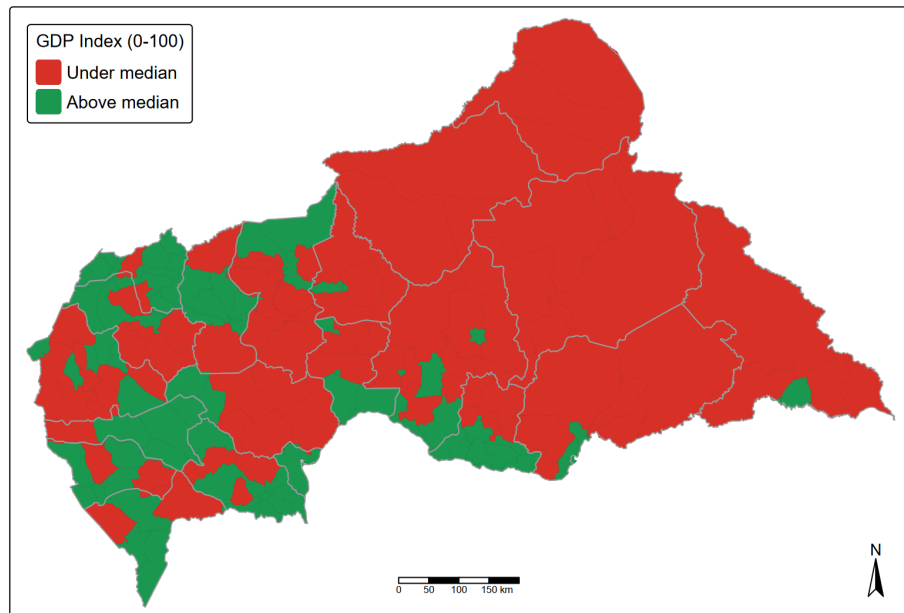
Overall vulnerability



*Source:* Authors' construction. *Notes:* Communes serve as the spatial reference unit; blue (orange) indicates communes below (above) the national median vulnerability.

Figure A.2: GDP index at communal level

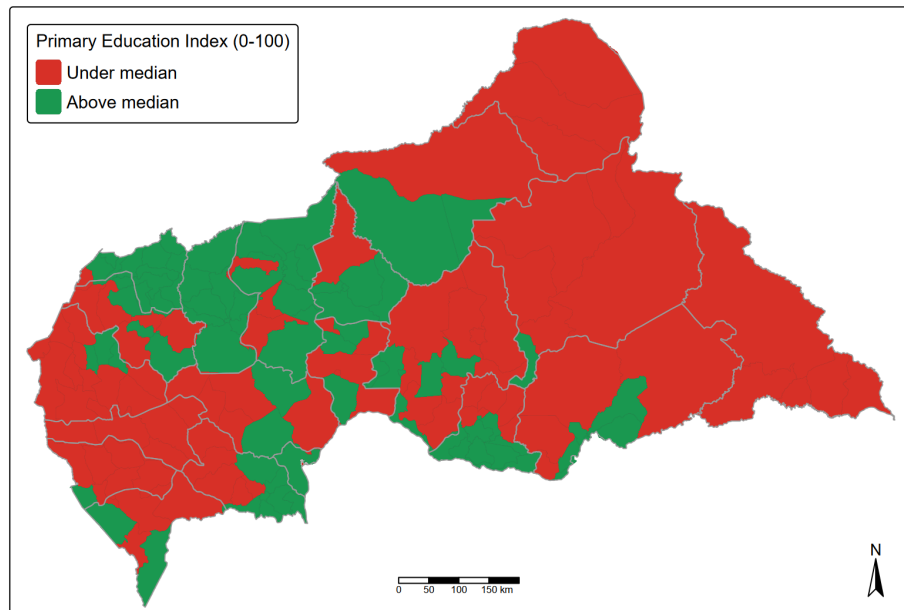
Total GDP Index, 2021



Source: Authors' construction. Notes: Communes serve as the spatial reference unit; green (red) indicates communes above (below) the national median economic activity.

Figure A.3: Education access index at communal level

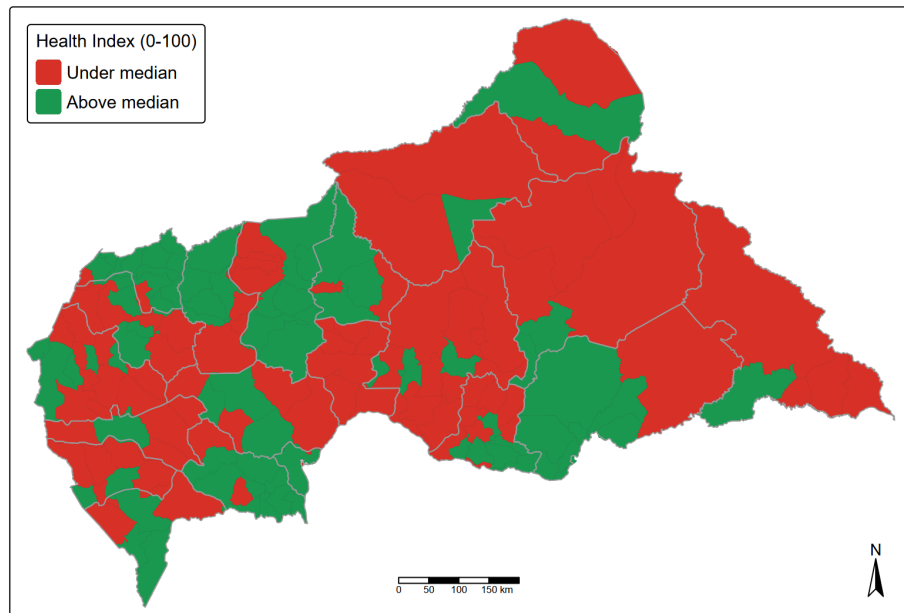
Access to primary education



Source: Authors' construction. Notes: Communes serve as the spatial reference unit; green (red) indicates communes above (below) the national median primary school access.

Figure A.4: Health access index at communal level

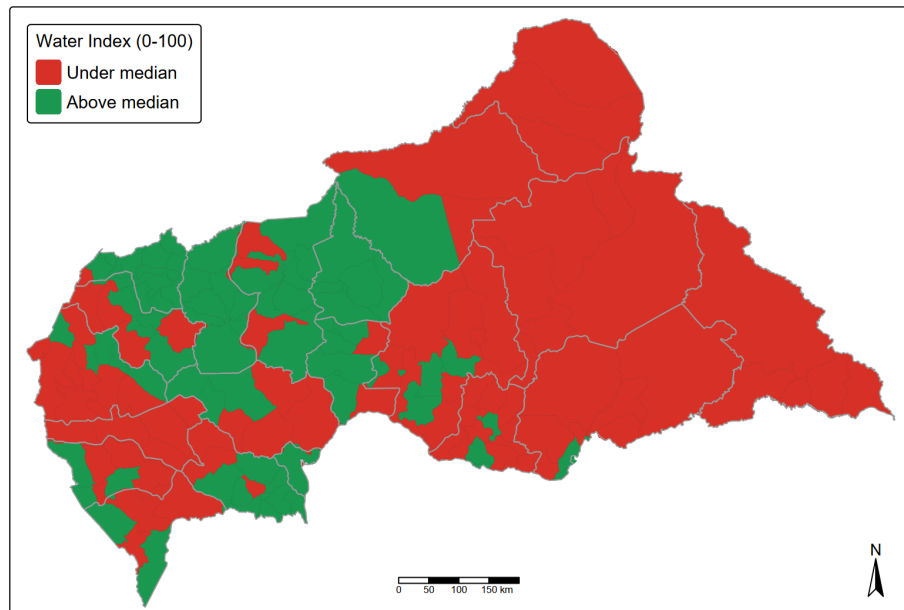
Access to any health facility



Source: Authors' construction. Notes: Communes serve as the spatial reference unit; green (red) indicates communes above (below) the national median health access.

Figure A.5: Water access index at communal level

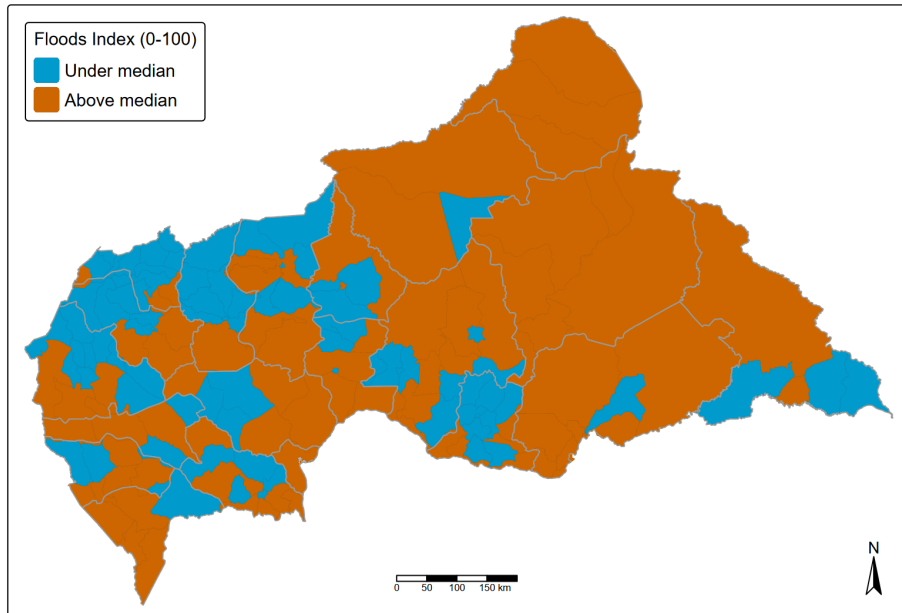
Access to water points



Source: Authors' construction. Notes: Communes serve as the spatial reference unit; green (red) indicates communes above (below) the national median water access.

Figure A.6: Floods index at communal level

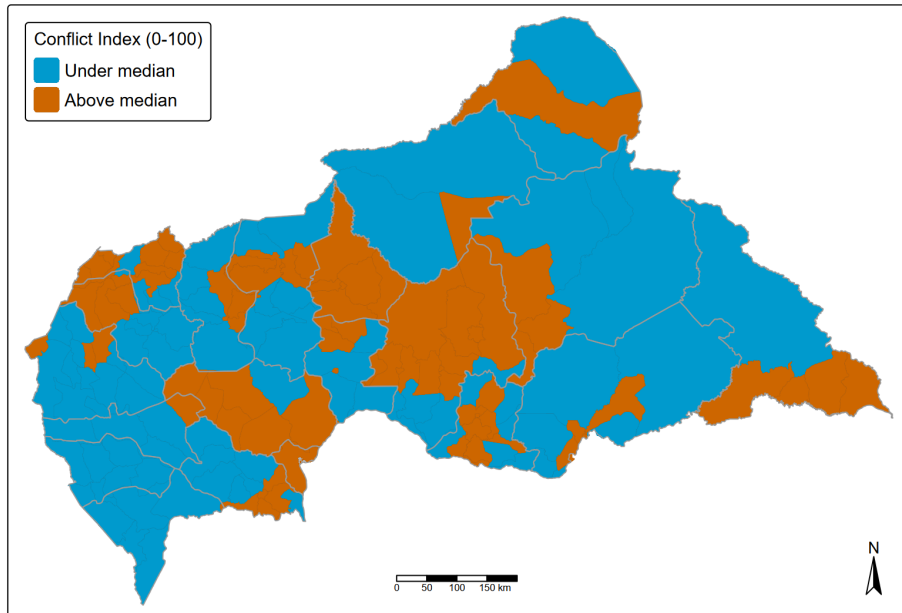
Flooding exposure



*Source:* Authors' construction. *Notes:* Communes serve as the spatial reference unit; blue (orange) indicates communes below (above) the national risk exposure to flooding.

Figure A.7: Lethal conflicts index at communal level

Conflict exposure



*Source:* Authors' construction. *Notes:* Communes serve as the spatial reference unit; blue (orange) indicates communes below (above) the national risk exposure to lethal conflicts.

### A.3 Robustness checks on survey validation

Tables A.2 and A.3 examine the robustness of the baseline results to disaggregation of GDP by economic sector. The primary sector GDP index demonstrates robust positive associations with household wealth across all specifications, with coefficients and maintaining statistical significance at conventional levels. In contrast, the secondary and tertiary sectors GDP index, while positive and significant in the basic specification, loses statistical significance once regional or prefectoral fixed effects are introduced. This differential pattern likely reflects the distinct spatial distributions of economic activities across CAR's territory. Secondary and tertiary sector activities concentrate predominantly in Bangui and a limited number of urban centers, generating strong spatial correlation with administrative boundaries that is likely absorbed by fixed effects. Primary sector activities, particularly subsistence agriculture, exhibit broader geographic distribution across rural areas, providing variation within administrative units that enables identification even with fixed effects controls.

Table A.2: Spatial vulnerability indices and household wealth: Basic services and economic activity disaggregated

	Households' baseline wealth index		
	Col.1	Col.2	Col.3
Primary GDP	1.519*** (0.447)	1.825** (0.449)	1.549* (0.567)
Secondary and Tertiary GDP	0.615*** (0.101)	0.130 (0.122)	0.167 (0.136)
Access to health index	0.014*** (0.002)	0.004 (0.002)	0.005* (0.002)
Access to primary education index	0.005*** (0.001)	0.006** (0.001)	0.005** (0.001)
Access to water index	0.013*** (0.001)	0.011*** (0.001)	0.011*** (0.001)
R2 Adj.	0.443	0.462	0.463
Num.Obs.	6,264	6,264	6,264
Covariates	Yes	Yes	Yes
Fixed effects	No	Regional	Prefectoral
Clustered standard errors	No	Yes	Yes

\* p < 0.05, \*\* p < 0.01, \*\*\* p < 0.001

*Source:* Authors' construction. *Notes:* Dependent variable is the household wealth index constructed following DHS methodology using EHCVM 2021 data. All spatial indices are measured at 5×5 km grid cell level and normalized on 0-100 scale. Indices for primary and secondary/tertiary GDP are constructed using remote sensing and geocoded data. Service access indices are derived from travel time to facilities and the density of associated infrastructure. Higher values mean higher local economic activities or better service access. Additional covariates—HH size; presence of IDPs in ordinary households or camps; whether the HH head is a woman; HH head's education level (primary, secondary first cycle, secondary second cycle, or higher); age of the HH head; and HH employment status (secondary sector, tertiary sector, or inactive/unemployed)—are included as controls but omitted from the table for brevity. Regional fixed effects account for the seven administrative regions of CAR, and prefectoral fixed effects control for the 20 prefectures. Standard errors are clustered at the regional level in Column (2) and the prefectoral level in Column (3). The sample comprises 6,264 households spatially matched to grid cells.

Table A.3: Spatial vulnerability indices and household wealth: Shock exposure and economic activity disaggregated

	Households' baseline wealth index		
	Col.1	Col.2	Col.3
Primary GDP Index	2.017*** (0.448)	2.100** (0.458)	1.495* (0.565)
Secondary and Tertiary GDP Index	0.503*** (0.102)	0.071 (0.123)	0.164 (0.135)
Floods index	0.027 (0.018)	0.003 (0.019)	0.011 (0.020)
Conflicts index	0.039*** (0.005)	0.029*** (0.004)	0.036*** (0.005)
R2 Adj.	0.443	0.461	0.463
Num.Obs.	6,264	6,264	6,264
Covariates	Yes	Yes	Yes
Fixed effects	No	Regional	Prefectoral
Clustered standard errors	No	Yes	Yes

\* p < 0.05, \*\* p < 0.01, \*\*\* p < 0.001

*Source:* Authors' construction. *Notes:* Dependent variable is the household wealth index constructed following DHS methodology using EHCVM 2021 data. All spatial indices are measured at 5×5 km grid cell level and normalized on 0-100 scale. Indices for primary and secondary/tertiary GDP are constructed using remote sensing and geocoded data. The risk indices measure physical exposure to flooding and lethal conflict, incorporating travel time to (potential) events. Higher values mean higher local economic activities or better service access. Additional covariates—HH size; presence of IDPs in ordinary households or camps; whether the HH head is a woman; HH head's education level (primary, secondary first cycle, secondary second cycle, or higher); age of the HH head; and HH employment status (secondary sector, tertiary sector, or inactive/unemployed)—are included as controls but omitted from the table for brevity. Regional fixed effects account for the seven administrative regions of CAR, and prefectoral fixed effects control for the 20 prefectures. Standard errors are clustered at the regional level in Column (2) and the prefectoral level in Column (3). The sample comprises 6,264 households spatially matched to grid cells.

Tables A.4 and A.5 assess robustness to alternative wealth index construction methodologies. Following DHS guidelines, this alternative specification employs distinct asset weighting procedures for urban and rural households to account for differential asset importance across spatial contexts. The complex wealth index construction recognizes that certain assets may serve different functions or carry different economic values in urban versus rural settings, necessitating context-specific weighting schemes. The validation results using this alternative wealth measure closely mirror the baseline findings in both coefficient magnitudes and statistical significance patterns. The stability of findings across alternative wealth measurement approaches strengthens confidence in the spatial vulnerability indices' validity and suggests that the observed relationships reflect genuine associations between spatial conditions and household welfare rather than artifacts of particular measurement conventions.

Table A.4: Spatial vulnerability indices and household wealth: Basic Services and economic activity (Complex wealth measurement)

	Households' complex wealth index		
	Col.1	Col.2	Col.3
GDP	0.104*** (0.007)	0.052** (0.010)	0.052*** (0.010)
Access to health index	0.018*** (0.002)	0.008* (0.002)	0.010** (0.002)
Access to primary education index	0.004*** (0.001)	0.005** (0.001)	0.003** (0.001)
Access to water index	0.004*** (0.001)	0.004* (0.001)	0.004** (0.001)
R2 Adj.	0.450	0.469	0.469
Num.Obs.	6,264	6,264	6,264
Covariates	Yes	Yes	Yes
Fixed effects	No	Regional	Prefectoral
Clustered standard errors	No	Yes	Yes

\* p < 0.05, \*\* p < 0.01, \*\*\* p < 0.001

*Source:* Authors' construction. *Notes:* Dependent variable is the household wealth index constructed following DHS methodology using EHCVM 2021 data. All spatial indices are measured at 5×5 km grid cell level and normalized on 0-100 scale. The GDP index is constructed using relevant remote sensing and geocoded data. Service access indices are derived from travel time to facilities and the density of associated infrastructure. Higher values mean higher local economic activities or better service access. Additional covariates—HH size; presence of IDPs in ordinary households or camps; whether the HH head is a woman; HH head's education level (primary, secondary first cycle, secondary second cycle, or higher); age of the HH head; and HH employment status (secondary sector, tertiary sector, or inactive/unemployed)—are included as controls but omitted from the table for brevity. Regional fixed effects account for the seven administrative regions of CAR, and prefectoral fixed effects control for the 20 prefectures. Standard errors are clustered at the regional level in Column (2) and the prefectoral level in Column (3). The sample comprises 6,264 households spatially matched to grid cells.

Table A.5: Spatial vulnerability indices and household wealth: Shock exposure and economic activity (Complex wealth measurement)

	Households' Complex wealth index		
	Col.1	Col.2	Col.3
GDP	0.101*** (0.007)	0.053** (0.010)	0.052*** (0.010)
Floods index	0.050** (0.019)	0.019 (0.020)	0.026 (0.020)
Conflicts index	0.040*** (0.005)	0.027*** (0.005)	0.033*** (0.005)
R2 Adj.	0.452	0.470	0.470
Num.Obs.	6,264	6,264	6,264
Covariates	Yes	Yes	Yes
Fixed effects	No	Regional	Prefectoral
Clustered standard errors	No	Yes	Yes

\* p < 0.05, \*\* p < 0.01, \*\*\* p < 0.001

*Source:* Authors' construction. *Notes:* Dependent variable is the household wealth index constructed following DHS methodology using EHCVM 2021 data. All spatial indices are measured at 5×5 km grid cell level and normalized on 0-100 scale. The GDP index is constructed from remote sensing and geocoded data. The risk indices measure physical exposure to flooding and lethal conflict, incorporating travel time to (potential) events. Higher values mean higher local economic activities or better service access. Additional covariates—HH size; presence of IDPs in ordinary households or camps; whether the HH head is a woman; HH head's education level (primary, secondary first cycle, secondary second cycle, or higher); age of the HH head; and HH employment status (secondary sector, tertiary sector, or inactive/unemployed)—are included as controls but omitted from the table for brevity. Regional fixed effects account for the seven administrative regions of CAR, and prefectoral fixed effects control for the 20 prefectures. Standard errors are clustered at the regional level in Column (2) and the prefectoral level in Column (3). The sample comprises 6,264 households spatially matched to grid cells.